



DOI: 10.34910/MCE.102.15

Dynamic response of structures located in near-field and far-field regions using IDA and MIDA

H.R. Mehdipanah, N. Fanaie*

K.N. Toosi University of Technology, Tehran, Iran

**E-mail: fanaie@kntu.ac.ir*

Keywords: modal incremental dynamic analysis (MIDA), incremental dynamic analysis (IDA), 3D model, irregularity in plan, near-field, far-field

Abstract. In the current research project, an effort is made so as to investigate the capability of the innovative Modal Incremental Dynamic Analysis (MIDA) method considering 3D structural models, the effect of plan irregularities and near-field earthquake records. Therefore, to fulfil this goal, 10 near-field earthquake records in one principal direction of structures as well as 10 far-field earthquake records in two principal directions of structures are applied to 12 structures with 6, 12 and 18-storeys, and 10 %, 20 %, 30 % and 40 % plan irregularities. The study of these parameters reveals that in geometrically regular 3D structures, this innovative method meets all seismic demands parameters just as the IDA method does. Furthermore, it concludes that MIDA method is not capable of obtaining the exact IDA curves in low-rise and medium-rise structures located in near-field regions since it results in noticeable errors. Finally, it is essential to improve the MIDA approach for near-field earthquake records by replacing the drift criterion utilized in this method with a more accurate drift criterion.

1. Introduction

Owing to severe earthquakes, analytical methods for evaluating the capacity of structures have dramatically changed over the years. As a result of exposure to severe earthquakes, structural elements exceed the yield point and enter into the plastic region. To better understand the dynamic behavior of structures, researchers need to evaluate the demand and capacity parameters accurately. For a long time, the behavior of structures had been studied through linear analysis, but this method has its own drawbacks such as overlooking the effect of higher modes and not being dynamic, to name but a few, which results in the structures being overdesigned. Due to special patterns of pushing such as uniform and mode shape based patterns, this method is not capable of meeting the exact demands of structures, when subjected to earthquakes. This problem caused all researchers to accept that nonlinear dynamic "Time-History" analysis can show the realistic behavior of structures. The merit of pushover analysis is that all stages from elastic to plastic behavior of the elements, which leads to instability of structure in the final stage, are monitored. On the other hand, nonlinear time-history dynamic analysis has showed the realistic behavior of structures. As a result, Incremental Dynamic Analysis, which was built based on the clusters of a large number of "Time History" analyses, was invented by Bertero [1]. This method simultaneously combined the advantages of both pushover and nonlinear time-history dynamic analyses. The structures were exposed to different scaled levels of Time-History earthquake records to observe elastic and plastic behavior as well as instability of all structural elements. Therefore, the structure's capacity is determined in different scaled levels. After Bertero, researchers, including Nassar and Krawinkler [2], Bazzurro and Cornell [3], Sameh Samir Mehanny and Gregory G. Deierlein [4], Gutpa and Kunnath [5] followed him; and in 2002, Vamvatsikos and Cornell [6] carried out invaluable survey on IDA method.

IDA is one of the most accurate methods for evaluating the dynamic behavior of structures. This method has been used by many researchers [7–9]. However, one of the worst drawbacks of this method is that it is time-consuming. For years, this has been a huge problem for researchers. From 1970 to 2000's there was a dire need for developing a new method to tackle this problem. Therefore, a numerical method named Modal



Incremental Dynamic Analysis (MIDA) capable of obtaining capacity and demand curves in less time than IDA emerged.

First attempt for solving problems was carried out by Vamvatsikos and Cornell in 2005 [6]. Zarfam and Mofid and Raiesi Fard in 2005 [10] proposed an approximate method named modal incremental nonlinear dynamic analysis. Han and Chopra in 2006 [11], offered a method, which was working on modal pushover based on IDA method. An innovative idea for estimating pushover curves based on error distribution was introduced by Mofid and Zarfam in 2008 [12]. Furthermore, the total input energy applied to SDOF oscillator was used as intensity measure to impose different levels of scaled earthquakes [12]. In another attempt in 2011, Zarfam and Mofid modified this method for those structures in which the elements' materials do not comply with bilinear behavior [13]. In the mentioned field, according to the study done by Jalilkhani and Manafpour, the method proposed by Shafei et al. [14] can confidently be employed as an efficient analysis tool for estimating the median seismic collapse capacity of RC frames [15]. As a last attempt, Mofid et al. modified MIDA in 2017 to investigate the seismic behavior of structures equipped with self-centering viscoelastic damper [16]. In 2017, Incremental Modal Pushover Analysis (IMPA) was proposed by Bergami et al. [17]. They concluded that IMPA approach cannot be considered as an alternative for IDA [17]. In all studies carried out by Mofid et al., they believed that MIDA results were accurate enough [10]. It should be mentioned that all the aforementioned researchers performed their survey on 2D frame using far-field earthquake records [10, 12, 13, 16]. Since real structures are mostly 3D with some irregularities in plan, there is a crucial need to investigate the accuracy of this method on these structures. Since near-field earthquake records feature pulse shape behavior and the frequency content has dramatic impact on the results, it is indispensable to study them.

In this article, the object of research is investigating of MIDA method on 3D models with irregularities in plan. The Subject of this research is dynamic response of these models located in near-field and far-field regions using MIDA Method.

The goal of present work is to investigate the accuracy of MIDA method in comparison to IDA.

2. Methods

Firstly, MIDA method will be reviewed. After that, the modeling and verifications of models will be described. Finally, the procedure of records selection and the way of performing the analysis will be explained.

2.1. Review on MIDA method

In the previous part, it was mentioned that the basic procedure of all surveys was based on the flowcharts presented in 2005 [10] and 2011 [12] by Zarfam and Mofid. This procedure is presented once again herein:

1. Modeling and designing of the structure.
2. Calculating the modes period and participation factor.
3. Performing pushover analysis, and obtaining pushover curve of i^{th} mode.
4. Is there negative hardening in pushover curve? If the answer is negative, construct the bi-linear behavior from obtained pushover curve according to Mofid et al. (2005) [10]; If the answer is positive, construct the trilinear behavior from obtained pushover curve according to Mofid et al. (2011) [12].
5. Modeling a SDOF system as below [10]:
 - a. The period of i^{th} mode in multi degree of freedom (MDOF) and SDOF must be even.
 - b. The damping of i^{th} mode in MDOF and SDOF must be even.
 - c. The yielding strength of i^{th} mode in MDOF and SDOF must have a relation.

$$(F_{yi})_{SDF} = (F_{yi})_{MDF} / (L/M)_i \quad (1)$$

The yielding displacement of i^{th} mode in MDOF and SDOF must have a relation.

$$(D_{yi})_{SDF} = (D_{yi})_{MDF} / [(L/M)_i \phi_{ri}] \quad (2)$$

The strain hardening angle (α) of i^{th} mode in MDOF and SDOF must be even.

$$\alpha_{SDF} = \alpha_{MDF} \quad (3)$$

where F_{yi} is yielding strength of the i^{th} mode of vibration;

D_{yri} is yielding displacement of the roof of the i^{th} mode of vibration;

α is the strain-hardening angle of the material;

ϕ_{ri} is the i^{th} roof mode shape;

And also,

$$L_i = \sum m_j \phi_{ji} \quad (4)$$

$$M_i = \sum m_j \phi_{ji}^2 \quad (5)$$

6. Exert n^{th} scaled level of earthquake to SDOF system to obtain maximum displacement.
7. Convert the maximum displacement of SDOF to MDOF as mentioned in the work by Zarfam and Mofid (2005) [10].
8. Push MDOF structure to converted maximum displacement and calculate the maximum drift in i^{th} mode
9. If the structure is stable, increase one level to scaled level of earthquake, if not, should another mode be considered? If the answer is yes, go to step 1, If not, go to step 10.
10. Compute the final maximum displacement and maximum drift of applied mode with SRSS method.
11. The MIDA curve is obtained.

2.2. Modeling and the assumptions of the models

In the 2nd type of irregularity mentioned in the table 12.3-1 of ASCE7-10, it is stated that "Reentrant corner irregularity" is defined to exist where both plan projections of the structure beyond a reentrant corner are greater than 15 % of the plan dimension of the structure in the given direction [18]. It means that when $X/L > 0.15$ and $Y/L' > 0.15$ occurred simultaneously, the structure is referred to as irregular. In this article 10 % projection simultaneously in both directions is considered as regular; on the other hand, 20 %, 30 % and 40 % projection in both directions are defined as irregular. In each of the principal directions, three spans with a length of 5 meters were considered. Three types of height, including 6, 12 and 18 stories were considered for the structures. As depicted in Fig. 1, plan of all structures is the same. Moreover, the height of each storey is assumed to be 3 meters, the construction location is in California, USA and the type of soil classification is assumed to be "C". Dead, live, and seismic loading applied to the structures comply with ASCE7.

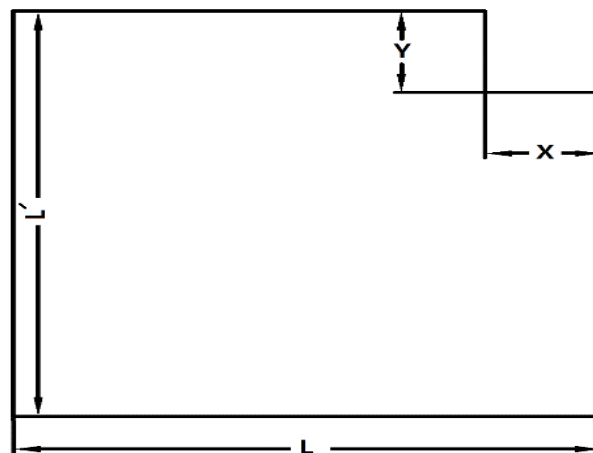


Figure 1. All structure plan.

All 12 structures were designed according to AISC 360-10 [19]. Weak beam-strong column criterion is observed in every single element of structures. All allowable drifts were satisfied in all structures.

Implementing IDA method, all structures need to be modeled in ETABS software and OpenSees. For this purpose, all elements were modeled as nonlinear-beam-column in OpenSees. All cross-sections were constructed by "patch quad" syntax. ST37 in OpenSees were modeled by "Steel02" material behavior. $P - \Delta$ effect was applied in OpenSees by local to global transformation order. All diaphragms and gravity loading were constructed similar to ETABS.

2.3. Verification

In this survey in order to verify the obtained results, two types of verifications were implemented as mentioned below:

2.3.1. Verification with regard to calculated periods

Periods obtained from ETABS and OpenSees must have rational exactness to assure that these two modelings represent the same model. Due to the large number of models, only a few of models have been included in this article. Here, EPeriod is the period obtained from ETABS; and OPeriod is the period obtained from OpenSees.

Table 1. Period verification in 12-story structures.

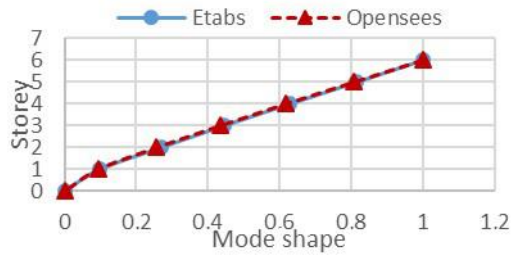
Irregularity percent		10%				20%			
Mode	EPeriod (s)	OPeriod (s)	Diff (s)	Ratio (%)	EPeriod (s)	OPeriod (s)	Diff(s)	Ratio (%)	
1 st	1.470	1.383	0.087	5.94	1.292	1.278	0.013	1.04	
2 nd	1.455	1.339	0.116	7.99	1.254	1.230	0.024	1.88	
4 th	0.549	0.528	0.021	3.86	0.489	0.495	0.007	1.38	
5 th	0.545	0.515	0.030	5.51	0.474	0.462	0.011	2.42	
7 th	0.315	0.309	0.006	1.79	0.276	0.288	0.012	4.33	
8 th	0.309	0.292	0.017	5.61	0.267	0.264	0.003	1.14	
Irregularity percent		30%				40%			
Mode	EPeriod (s)	OPeriod (s)	Diff(s)	Ratio (%)	EPeriod (s)	OPeriod (s)	Diff(s)	Ratio (%)	
1 st	1.277	1.249	0.027	2.15	1.155	1.127	0.028	2.44	
2 nd	1.269	1.241	0.028	2.18	1.127	1.111	0.015	1.35	
4 th	0.487	0.492	0.005	0.94	0.440	0.440	0.000	0.05	
5 th	0.483	0.483	0.000	0.10	0.434	0.428	0.005	1.19	
7 th	0.279	0.287	0.007	2.66	0.259	0.265	0.006	2.20	
8 th	0.278	0.281	0.003	1.12	0.257	0.253	0.003	1.29	

Table 2. Period verification in 18-story structures.

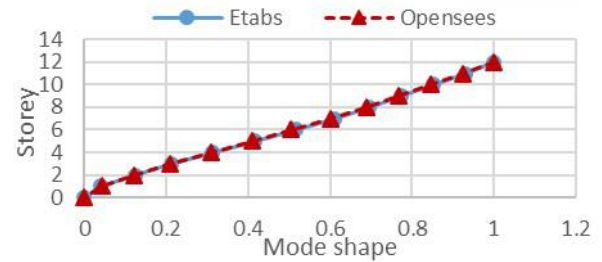
Irregularity percent		10%				20%			
Mode	EPeriod (s)	OPeriod (s)	Diff (s)	Ratio (%)	EPeriod (s)	OPeriod (s)	Diff (s)	Ratio (%)	
1 st	2.181	2.074	0.106	4.88	1.770	1.725	0.045	2.56	
2 nd	2.164	2.009	0.156	7.20	1.720	1.668	0.052	3.02	
4 th	0.817	0.834	0.017	2.10	0.637	0.625	0.012	1.91	
5 th	0.802	0.773	0.029	3.59	0.630	0.603	0.027	4.27	
7 th	0.478	0.490	0.012	2.40	0.379	0.386	0.007	1.77	
8 th	0.471	0.460	0.011	2.35	0.372	0.362	0.010	2.71	
Irregularity percent		30%				40%			
Mode	EPeriod (s)	OPeriod (s)	Diff (s)	Ratio (%)	EPeriod (s)	OPeriod (s)	Diff(s)	Ratio (%)	
1 st	1.845	1.839	0.006	0.30	1.752	1.798	0.047	2.65	
2 nd	1.828	1.815	0.013	0.69	1.695	1.759	0.064	3.79	
4 th	0.680	0.685	0.004	0.62	0.615	0.620	0.006	0.92	
5 th	0.678	0.680	0.002	0.33	0.599	0.608	0.009	1.59	
7 th	0.411	0.417	0.006	1.47	0.363	0.365	0.002	0.65	
8 th	0.409	0.415	0.006	1.44	0.357	0.356	0.002	0.42	

2.3.2. Mode shape verification

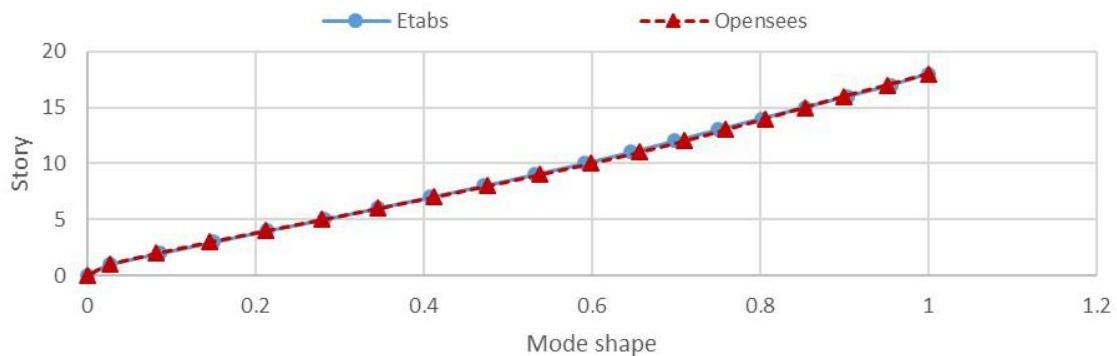
To make sure that all the aforementioned 12 structures are accurately built in ETABS, there was a crucial need to verify that all elements were correctly assigned. In period verification, accidental errors may offset each other and make all periods correct, but in essence these structures are different from each other. For this reason, it is essential to implement shape mode verification. By doing this, any mismatches in stiffness or mass in each individual storey would be tackled.



a. Mode shape verification of 6 storey structure with 40% irregularity on the first mode in Y direction



b. Mode shape verification of 12 storey structure with 10% irregularity on the first mode in X direction



c. Mode shape verification of 18 storey structure with 20% irregularity on the first mode in Y direction

Figure 2. Three samples of mode shapes verifications of structures for better understanding.

Fig. 2(a), (b) and (c) represent overlapping of first mode shape in X direction in 6 storey structure, first mode shape in Y direction in 12 storey structure and first mode shape in Y direction in 18 storey structure, all obtained by ETABS and OpenSees, respectively.

2.4. Record selection

While selecting appropriate records for this study, some recommendations in near-field and far-field region need to be followed.

2.4.1. Selecting near-field records

For selecting near-field records, there are some recommendations provided by FEMA P695, 2009, which is obligatory to comply [20]. These recommendations are outlined below:

1. Soil classification of the records must be the same as the one on which the structures have been modeled.
2. The focal fault mechanism of records must be the same as the one on which the structures have been modeled.
3. The magnitude of records must be equal or higher than 6 Richter to avoid mistakenly selecting an aftershock.
4. Peak ground acceleration must be higher than 0.6g.
5. To select the certifiably near-field records, R_{jb} and R_{rup} must be less than 10 km. R_{jb} is the Joyner-Boore distance which is defined as the closest horizontal distance to the surface projection of the fault plane. Also, R_{rup} is the closest distance to the coseismic rupture plane (km).
6. Pulse behavior should be perceived in velocity versus time graph.

According to the aforementioned recommendations, strike-slip was chosen for focal mechanism and "C" soil type was assumed for selecting records. It should be mentioned that regarding these recommendations, some records were selected from FEMA P695 and the others were obtained from PEER website. The roster of selected records is listed in the following table.

Table 3. Near-field records list.

No.	Earthquake name	Year	Station Name	Mag	Mechanism	R_{jb} (km)	R_{rup} (km)	Vs 30 (m/sec)
1	Morgan Hill	1984	"Coyote Lake Dam - Southwest Abutment"	6.19	strike slip	0.18	0.53	561.43
2	Bam_ Iran	2003	"Bam"	6.6	strike slip	0.05	1.7	487.4
3	Parkfield	1966	Temblor pre-1969	6.19	strike slip	15.96	15.96	527.92
4	San Salvador	1986	"Geotech Investig Center"	5.8	strike slip	2.14	6.3	489.34
5	Mammoth Lakes-06	1980	Long Valley Dam (Upr L Abut)	5.94	strike slip	9.65	16.03	537.16
6	"Chi-Chi_ Taiwan-04"	1999	"CHY074"	6.2	strike slip	6.02	6.2	553.43
7	Coyote Lake	1979	Gilroy Array #6	5.7	strike slip	0.42	3.11	663.31
8	"Parkfield-02_ CA"	2004	"Parkfield - Cholame 3E"	6	strike slip	4.95	5.55	397.36
9	Kocaeli, Turkey	1999	Arcelik	7.51	strike slip	10.56	13.49	523
10	"Darfield_ New Zealand"	2010	"LPCC"	7	strike slip	25.21	25.67	649.67

Records number 1, 4, 5 and 7 are selected from the article of Dimakopoulo et al. (2013) [21]. Record number 3 is selected from Davoodi and Jafari [22]. The other records are selected with the help of recommendation obligated in FEMA P695 [20].

2.4.2. Selecting far-field records

There are also some recommendations for selecting far-field records [20] which are listed below:

1. Soil type of the records must be the same as the one on which structures have been modeled.
2. The focal fault mechanism of records must be the same as the one on which structures have been modeled.
3. To appropriately select the near-field records R_{jb} and R_{rup} must be more than 15 km.

Based on the FEMA P695 recommendations, the far-field records roster is presented in the following table:

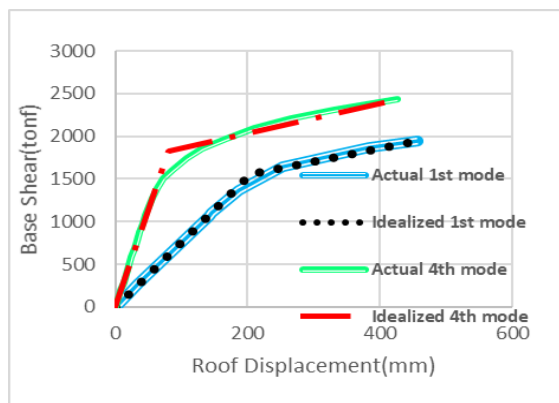
Table 4. Far-field records list.

No.	Earthquake Name	Year	Station Name	Mag.	Mechanism	R_{jb} (km)	R_{rup} (km)	Vs30 (m/s)
1	"Big Bear-01"	1992	"Snow Creek"	6.46	strike slip	37.04	38.07	523.59
2	"Tottori_ Japan"	2000	"OKY004"	6.61	strike slip	19.72	19.72	475.8
3	"Darfield_ New Zealand"	2010	"Heathcote Valley Primary School"	7	strike slip	24.36	24.47	422
4	"Victoria_ Mexico"	1980	"Cerro Prieto"	6.33	strike slip	13.8	14.37	471.53
5	"Landers"	1992	"Morongo Valley Fire Station"	7.28	strike slip	17.36	17.36	396.41
6	"Chi-Chi_ Taiwan-04"	1999	"CHY028"	6.2	strike slip	17.63	17.7	542.61

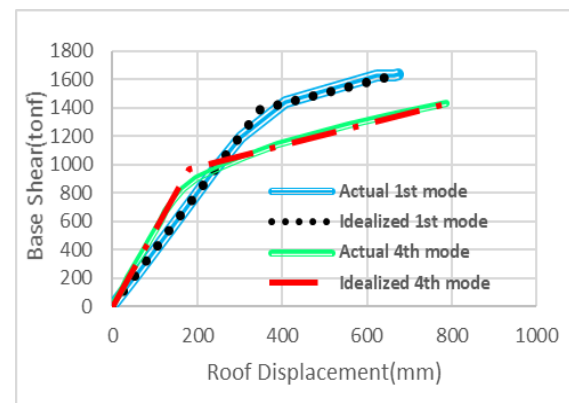
No.	Earthquake Name	Year	Station Name	Mag.	Mechanism	R_{jb} (km)	R_{rup} (km)	V_{s30} (m/s)
7	"Chalfant Valley-02"	1986	"Benton"	6.19	strike slip	21.55	21.92	370.94
8	"Joshua Tree_ CA"	1992	"Whitewater Trout Farm"	6.1	strike slip	28.97	29.4	425.02
9	"Imperial Valley-06"	1979	"Cerro Prieto"	6.53	strike slip	15.19	15.19	471.53
10	"Basso Tirreno_ Italy"	1978	"Naso"	6	strike slip	17.15	19.59	620.56

2.5. Performing analysis and obtaining curves

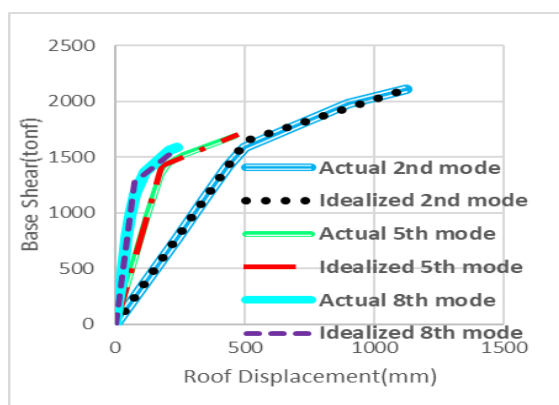
Achieving the purposes of this survey, firstly bilinear curves must be built according to recommendations in part 2. In order to obtain these curves, plastic hinges for performing pushover analysis based on FEMA365 [23] must be assigned to all elements. Then, structures are pushed to the maximum calculated displacement. Subsequently, plastic hinges are formed in beams at first stage; then, plastic hinges at the end of columns, which are rigidly connected to the base, were forged; these two steps of procedure cause structures to be unstable. In all three steps, by monitoring the displacements versus forces, pushover curves were obtained and bilinear curves were built using the procedure discussed in part 2. In this survey, these bilinear curves are specified using the rules of equality of areas above and below the capacity curve of pushover. To solve this problem with good precision, trapezoidal elements were implemented so as to get even areas.



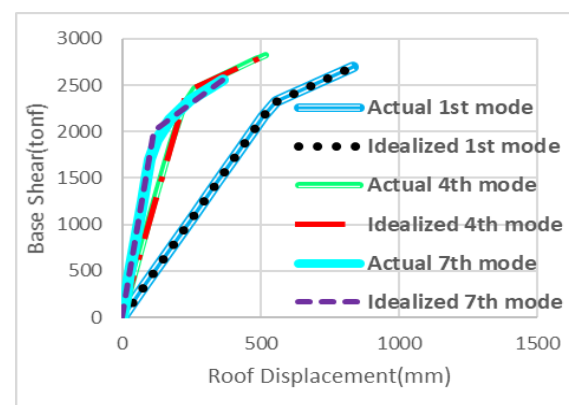
a. 6-storey structure with 20% irregularity



b. 12-storey structure with 10% irregularity



c. 18-storey structure with 20% irregularity



d. 18-storey structure with 40% irregularity

Figure 3. Matching the idealized pushover curve with actual one.

As Fig. 3 illustrates, there is a good conformity between the obtained capacity curves from ETABS and the idealized bilinear graphs revealing that all steps have been correctly employed. Consequently, by utilizing the modal information, these bilinear specifications are converted to the stress-strain diagram for SDOF systems. In the next steps of MIDA, these specifications are exerted for each individual mode of all 12 structures. In addition, all SDOF systems are modeled with complete requirements in OpenSees to perform analysis using near-field and far-field earthquake records. All SDOF systems include one mass and a massless spring, which need to comply with idealized stress-strain diagram specified for individual modes.

Due to the burden of extremely heavy numbers of analyses that need to be performed, the first two transitional modes in each direction for 6 and 12 storey structures are considered. For 18-storey structures, in order to see the effect of higher modes, the first three transitional modes in each direction were considered. All 12 structures are analyzed and subjected to 10 near-field earthquake records in one principal direction and 10 far-field earthquake records in two principal directions. In this survey, maximum displacement should be one of the damage indexes; and the other one, as the procedure dictates, needs to be the maximum roof drift. For better understanding, PGA was selected as intensity index so as to follow the procedure of the pioneers of this method. Then, after performing the analyses, maximum displacement for SDOF system obtained is turned into the maximum displacement of MDOF system to conduct pushover analysis on 3D models by the formulae presented in Zarfam and Mofid article [10]. Then, maximum drifts are obtained as per the procedure presented by Mofid et al. articles [10]; all drifts and displacements obtained from each response to the individual record excitation are gotten SRSS for plotting curves. For IDA and MIDA, 360 analyses were performed individually and respectively.

Due to extremely large number of graphs produced in this survey, the authors have decided to include some of them as well as a few comparison graphs, including graphs of “Morgan Hill” record for near-field region.

3. Results and Discussions

In part 3.1 results with comparison graphs have been presented. In addition, in part 3.2 authors discussed the results.

3.1. Results

Here, the comparison of MIDA and IDA graphs will be presented for far-filed and near field records. In addition, graphs, which demonstrate the effect of structures' height on MIDA method, will be illustrated at last part.

3.1.1. Comparison of maximum roof displacement and drift versus PGA under near-field records

Because of the extremely large number of graphs that were produced in this survey, the authors have decided to include some of them as well as a few comparison graphs, including graphs of “Morgan Hill” record for near-field region.

3.1.1.1. Comparison of maximum roof displacement and drift versus PGA in “Morgan Hill” record for 6-story structures

Comparison of maximum roof displacement and roof drift versus PGA in “Morgan Hill” record for 6-storey structures with irregularities from 10 % to 40 %.

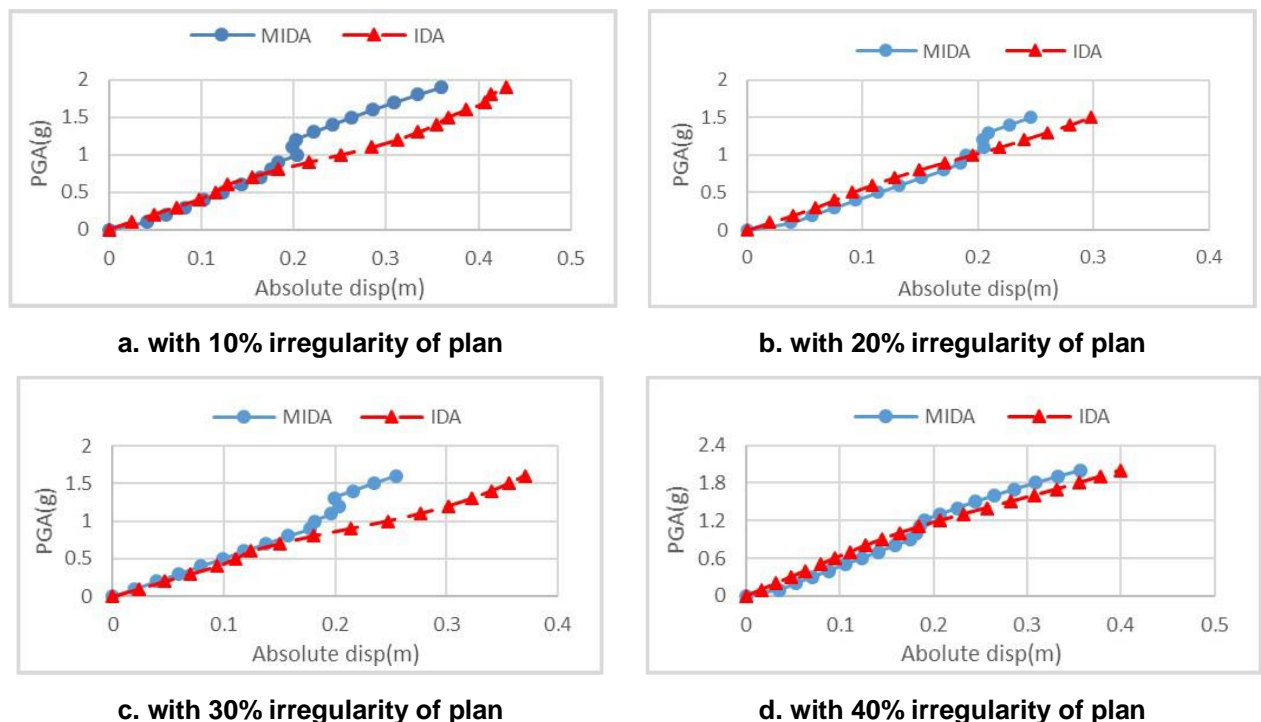


Figure 4. Comparison of roof displacement from IDA and MIDA methods in 6-storey structures for record No.1 in near-field records.

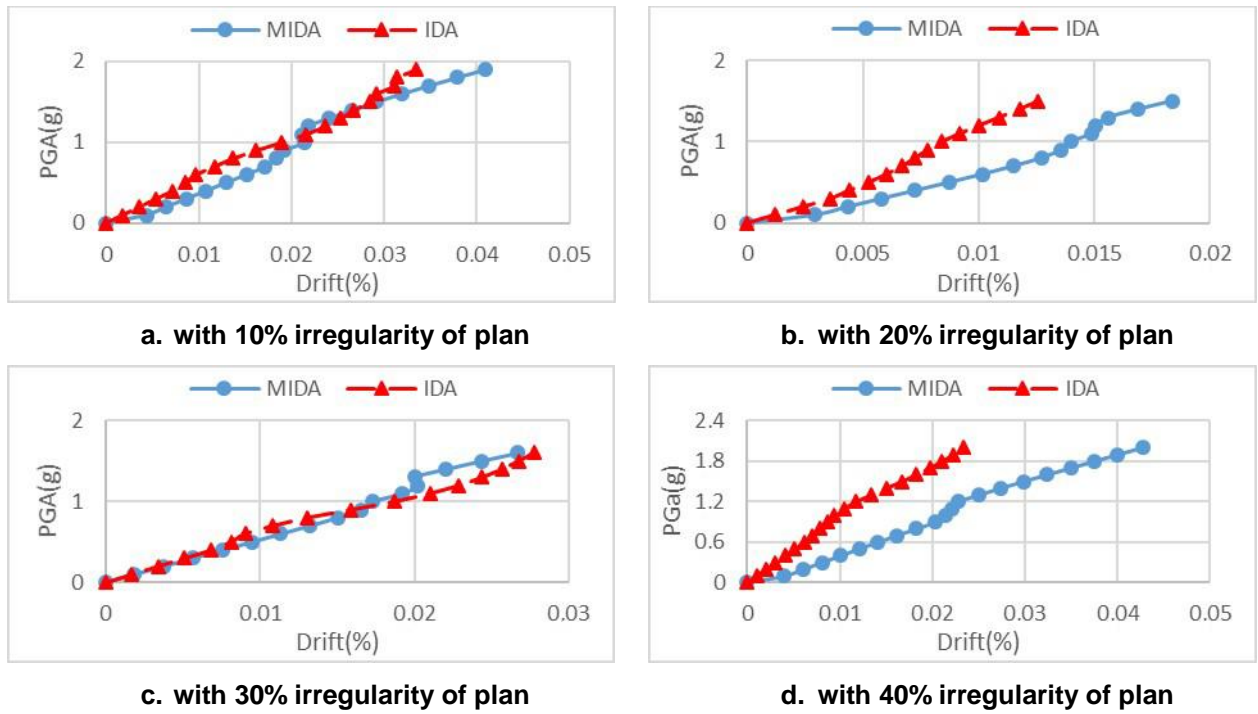


Figure 5. Comparison of roof drift from IDA and MIDA methods in 6-storey structures for record No.1 in near filed records.

Comparing the roof displacements obtained from these two methods, it is observed that MIDA is not precise enough in the analysis of low-rise buildings located in near field regions. From the comparison of roof drift in these two methods, it can be concluded that MIDA is not accurate enough in low-rise buildings located in near-field regions neither in elastic region nor in plastic one.

3.1.1.2. Comparison of maximum roof displacement and drift versus PGA in “Morgan Hill” record for 12-storey structures

Comparison of maximum roof displacement and drift versus PGA in “Morgan Hill” record for 12-storey structures with irregularities from 10 % to 40 %.

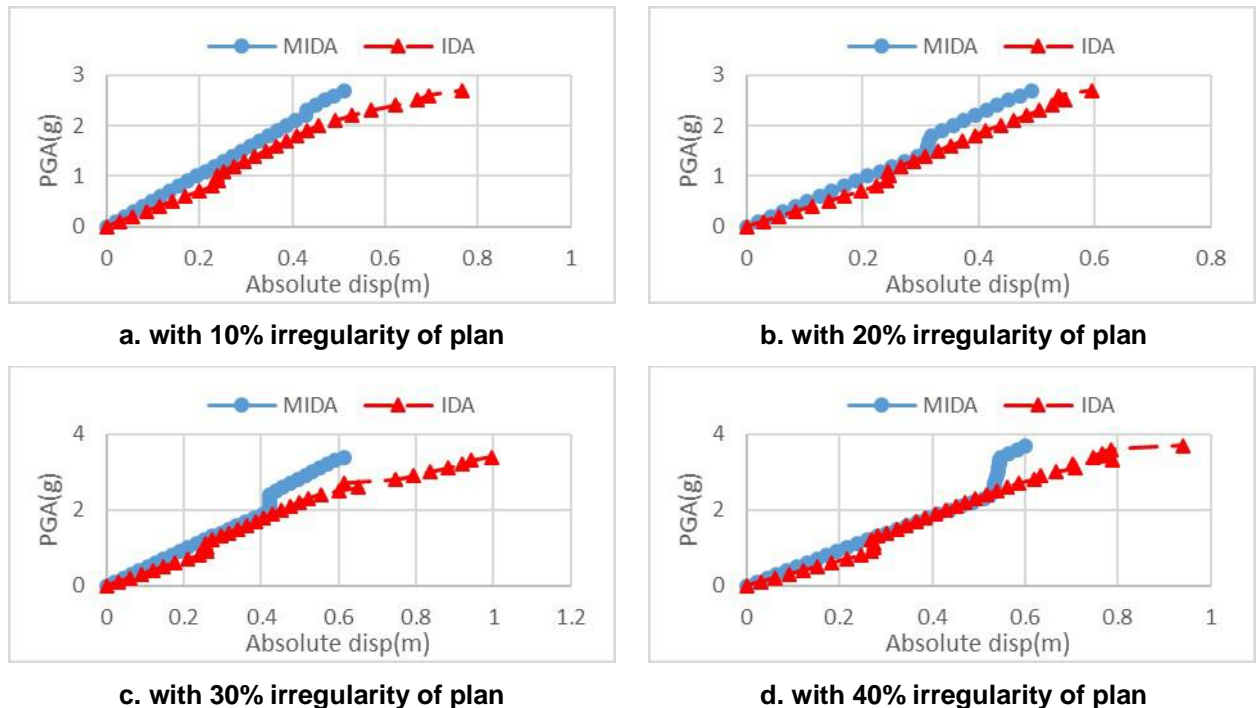


Figure 6. Comparison of roof displacement from IDA and MIDA methods in 12-storey structures for record No.1 in near field records.

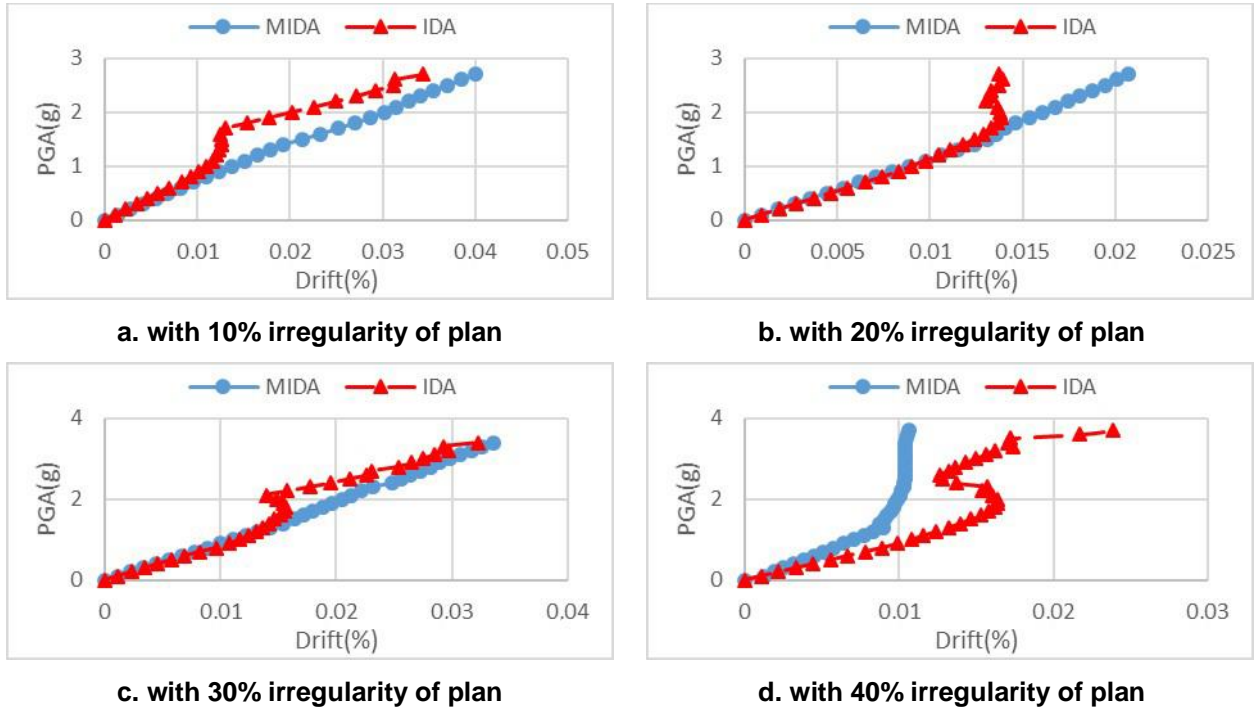


Figure 7. Comparison of roof drift from IDA and MIDA methods in 12-storey structures for record No.1 in near field records.

Comparing the roof displacements in these two methods, it can be seen that MIDA is not precise enough in near-field records on medium-rise buildings. From the comparison of roof drift in these two methods, it can be seen that MIDA method is not precise enough in near-field records on medium-rise buildings neither in elastic region nor in plastic one. It can be concluded that the increase in height of structures increases the errors by keeping fixed the number of modes for performing analysis.

3.1.1.3. Comparison of maximum roof displacement and drift versus PGA in “Morgan Hill” record for 18- storey structures

Comparison of maximum roof displacement and drift versus PGA in “Morgan Hill” record for 18- storey structures with irregularities from 10% to 40%.

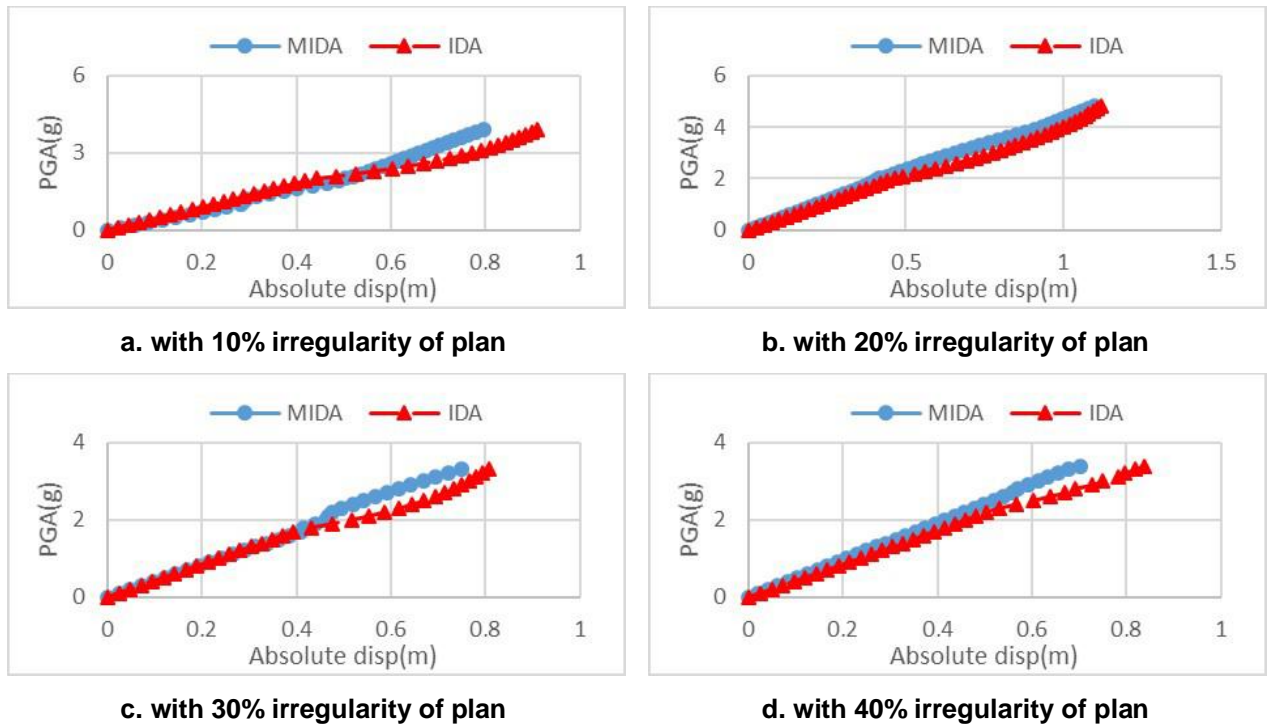


Figure 8. Comparison of roof displacement from IDA and MIDA methods in 18-storey structures for record No.1 in near field records.

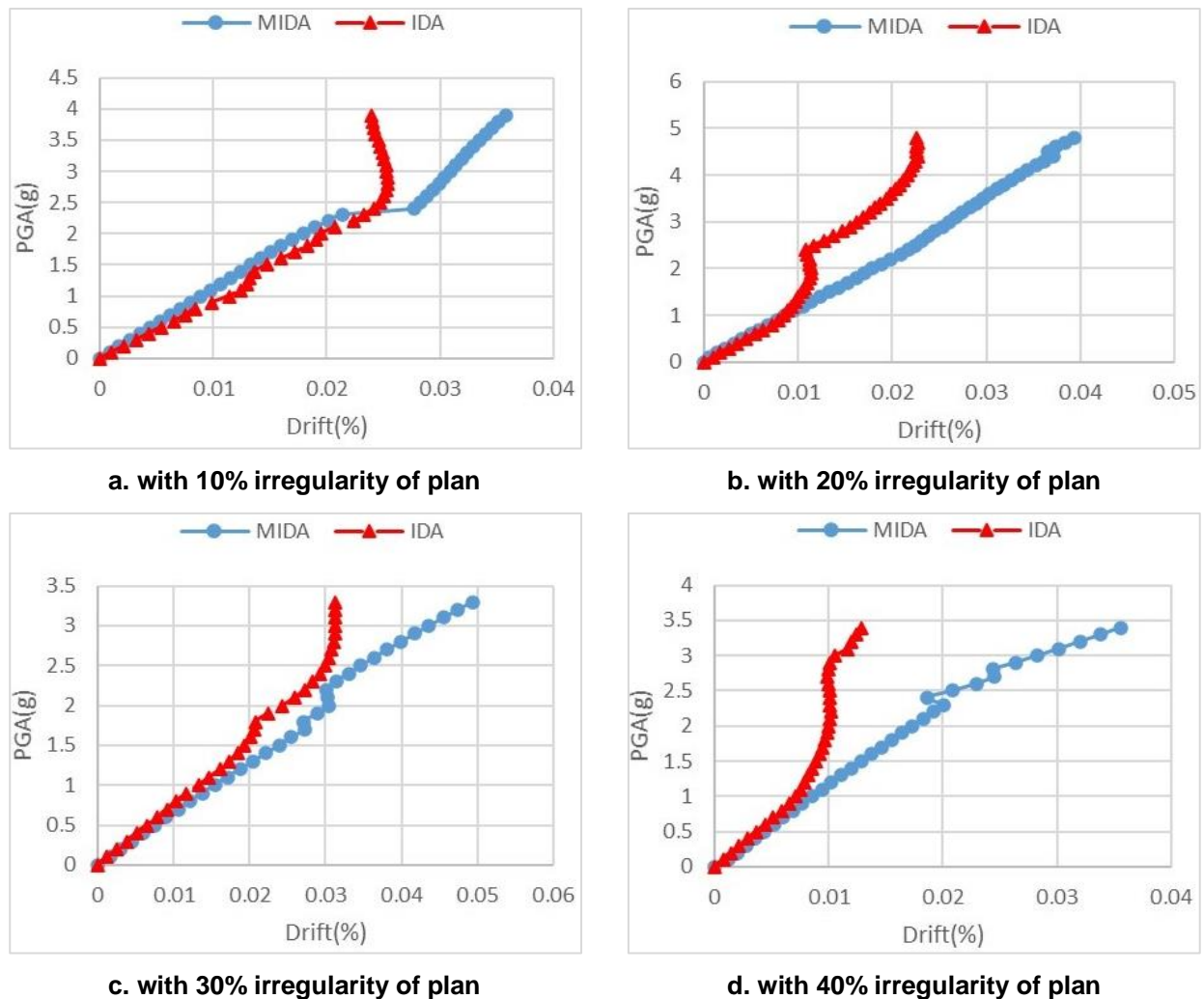


Figure 9. Comparison of roof drift from IDA and MIDA methods in 12-storey structures for record No.1 in near field records.

By comparing maximum roof displacement as well as maximum drift in these two methods as shown in Fig. 8 and 9, it can be concluded that the linear region of IDA method in 18-storey structures can be obtained by MIDA method. The reasoning lies in two things. Firstly, according to the survey carried out by Krawinkler et al. in 1999, spectra response of SDOF systems cannot satisfy seismic demands for near-field fault [24]. Secondly, MIDA method was based on SDOF system. Consequently, displacement and drift graph in low-rise and medium-rise structures cannot be obtained correctly and precisely. On the other hand, near-field earthquake records have a huge impact on low-rise and medium-rise structures; but 18-storey structures, as high-rise structures, are less affected by near-field earthquakes; accordingly, IDA and MIDA results match better to each other.

By passing the border of linear region in structural elements, they become plastic elements. Therefore, their stiffness changes result in changes in periods of structure. The validation of SRSS method is up to the point where modes do not interfere with each other. However, when structural elements become plastic and the period changes significantly, SRSS method is not valid anymore. Hence, this is one of the factors creating some errors in this method in inelastic region. In addition, figures illustrate that if the extent of irregularity increases, errors of this method dramatically increase because of the intense torsion of structure. Accumulation of plastic hinges in the reentrant corner of irregularity is the leading cause of this effect. Therefore, applicability of this method narrows down.

3.1.2. Comparison of maximum roof displacement and drift versus PGA in far-field records

Due to the extremely large numbers of graphs produced in this survey, the authors have decided to present comparison graphs of “Darfield _New Zealand” and “Chi- Chi_Tiwan-04” earthquake records for X direction and Y direction respectively in far-field records.

3.1.2.1. Comparison of maximum roof displacement and drift versus PGA for 6-storey structures

Comparison of maximum roof displacement and drift versus PGA in “Chi-Chi_Tiwan-04” earthquake record for Y direction in far-field records for 6-storey structures with irregularities from 10 % to 40 %.

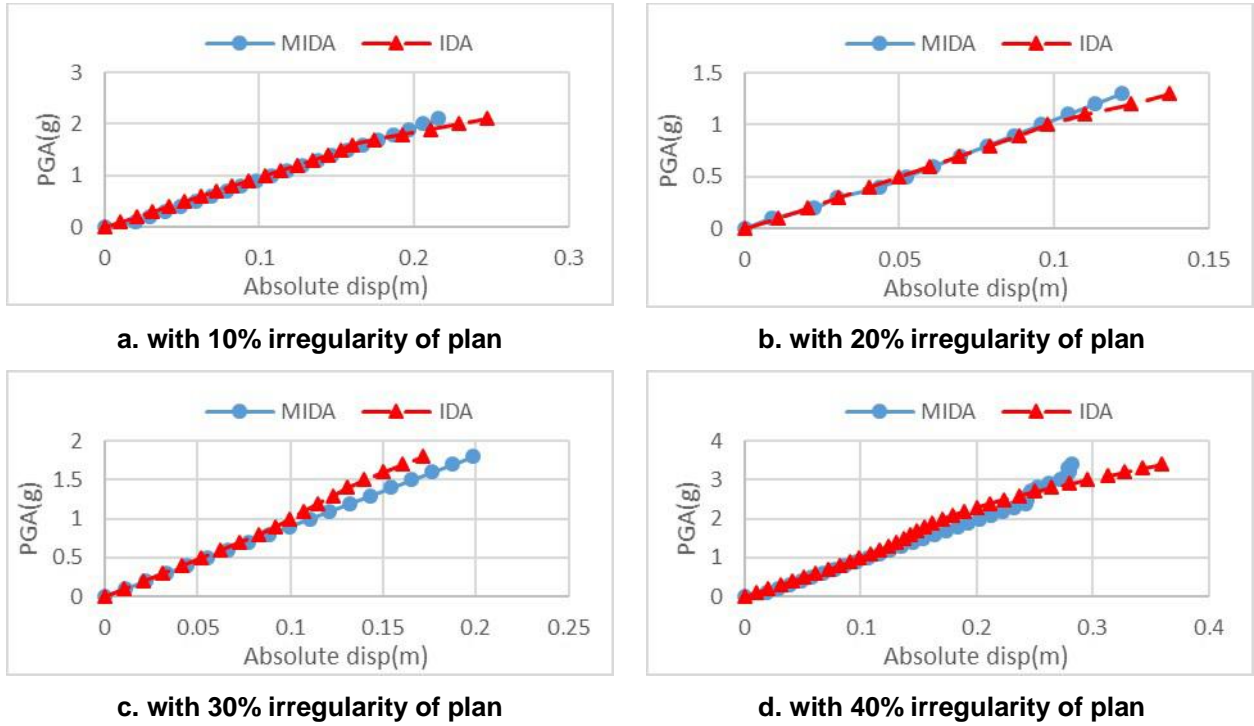


Figure 10. Comparison of roof displacement from IDA and MIDA methods in 6-storey structures under record No.3 in far field records Y-Direction.

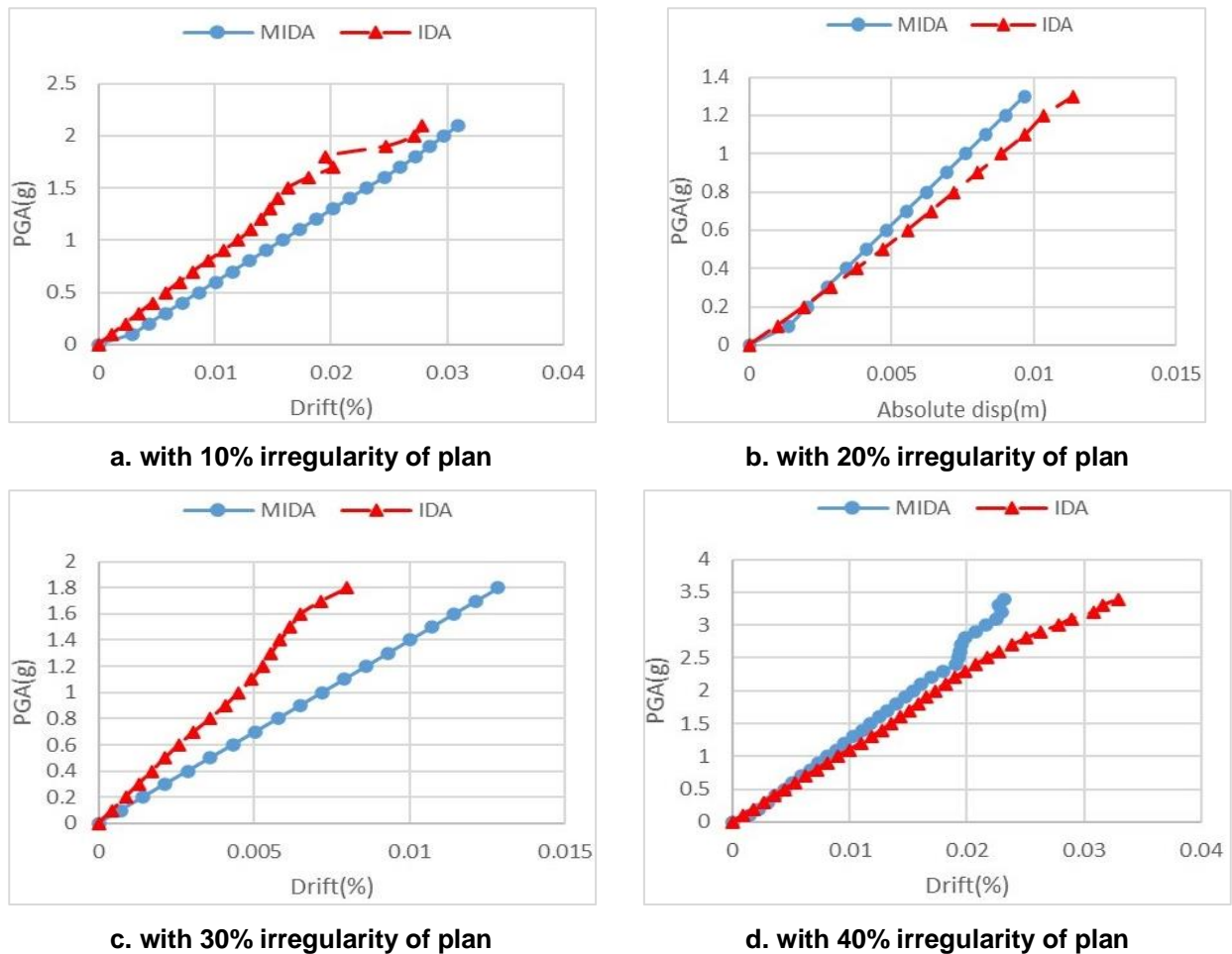


Figure 11. Comparison of roof drift from IDA and MIDA methods in 6-storey structures under record No.3 in far field records Y-Direction.

As Fig. 10 to Fig. 11 depict, MIDA method in both maximum roof displacement and maximum roof drift, is capable of extracting the accurate answer in linear region in far-field records. However, in nonlinear region, if the extent of intensity increases, errors of this method slightly increase in 6-storey structures. If the extent of

irregularity increases, errors of this method significantly increase because of the intense torsion of structure. Accumulation of plastic hinges in the reentrant corner of irregularity is the main cause of this effect. Therefore, applicability of this method decreases.

3.1.2.2. Comparison of maximum roof displacement and drift versus PGA 12-storey structures

Comparison of maximum roof displacement and drift versus PGA in “Darfield _New Zealand” earthquake record for X direction in far-field records for 12-storey structures with irregularities from 10 % to 40 %.

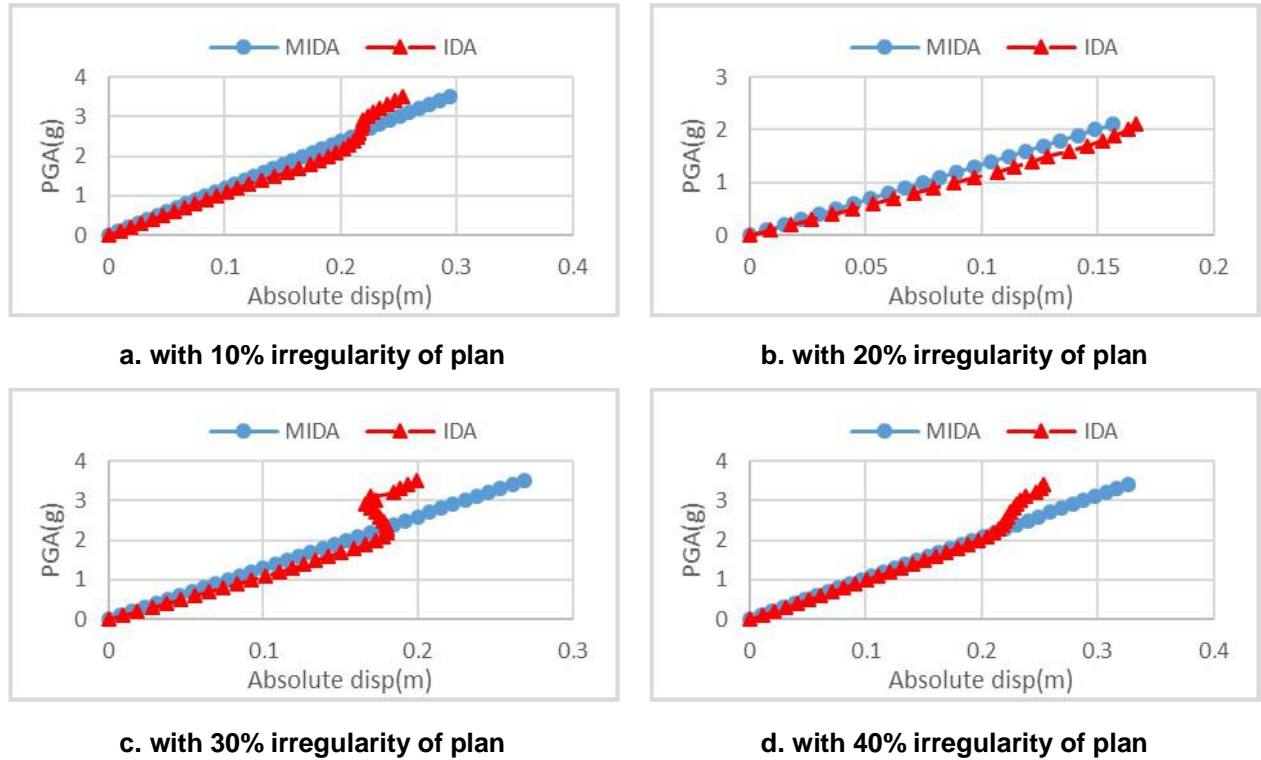


Figure 12. Comparison of roof displacement from IDA and MIDA methods in 12-storey structures under record No.3 in far field records X-Direction.

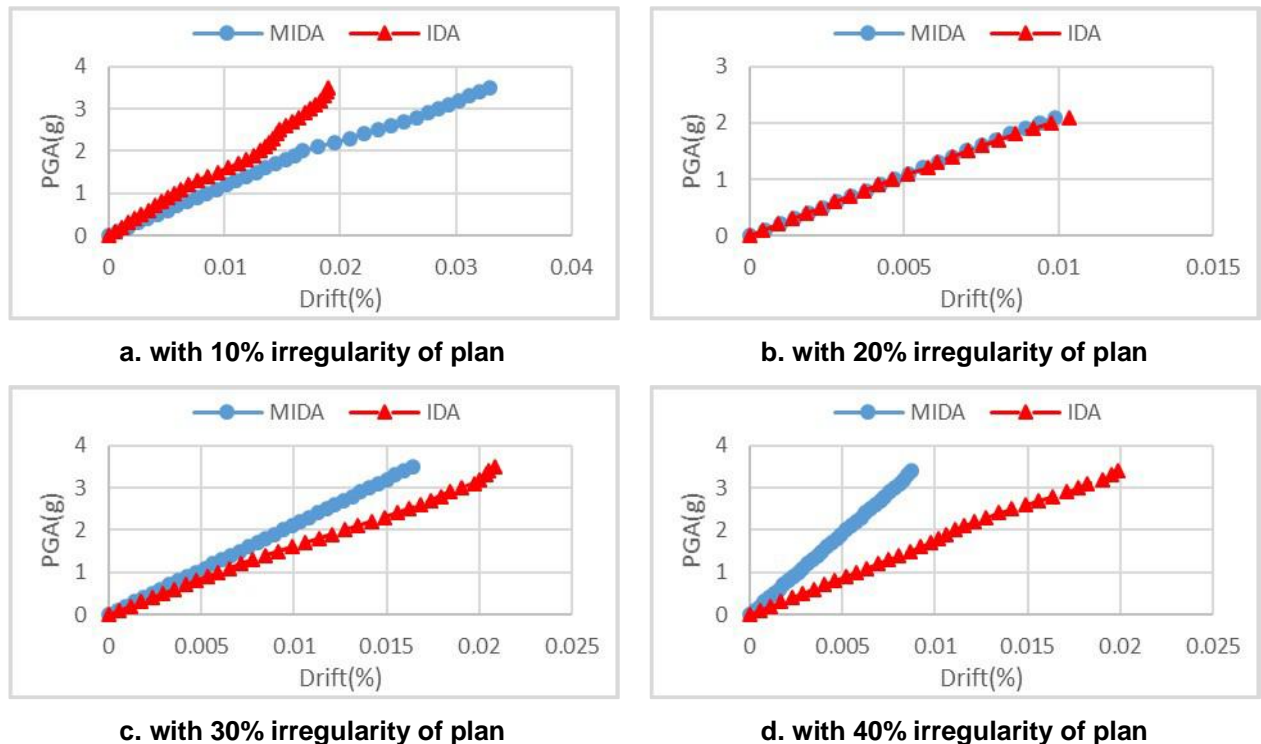


Figure 13. Comparison of roof drift from IDA and MIDA methods in 12-storey structures under record No.3 in far field records X-Direction.

As Fig. 12 to Fig. 13 depict, MIDA method, in both maximum roof displacement and maximum roof drift, is capable of extracting the precise answer in linear region in far-field records. However, in nonlinear region, if the extent of intensity increases, errors of this method slightly increase in 12-storey structures. By passing the border of linear region in structural elements, they become plastic elements. Therefore, their stiffness changes; consequently, the periods of structures change as well. The validation of SRSS method is when modes do not have interference with each other. However, when structural elements become plastic and period changes, SRSS method is not feasible anymore. Therefore, this is one of the factors, which brings about some errors in this method in inelastic region. In addition, figures illustrate that if the extent of irregularity increases, errors of this method significantly increase because of the intense torsion of structure. Accumulation of plastic hinges in the reentrant corner of irregularity is the main reason of this effect. Therefore, applicability of this method decreases. In addition, these errors are larger than those calculated in 6-storey structures. It is also mentioned that in 6, 12-storey structures, the number of modes considered for MIDA is the same. Therefore, it can be deduced that when the height of structures increases, the considered modes should increase by at least one more mode in order to decrease the errors in MIDA method.

3.1.2.3. Comparison of maximum roof displacement and drift versus PGA 18-storey structures

Comparison of maximum roof displacement and drift versus PGA in “Chi-Chi_Tiwan-04” earthquake record for Y direction in far-field records for 18-storey structures with irregularities from 10 % to 40 %

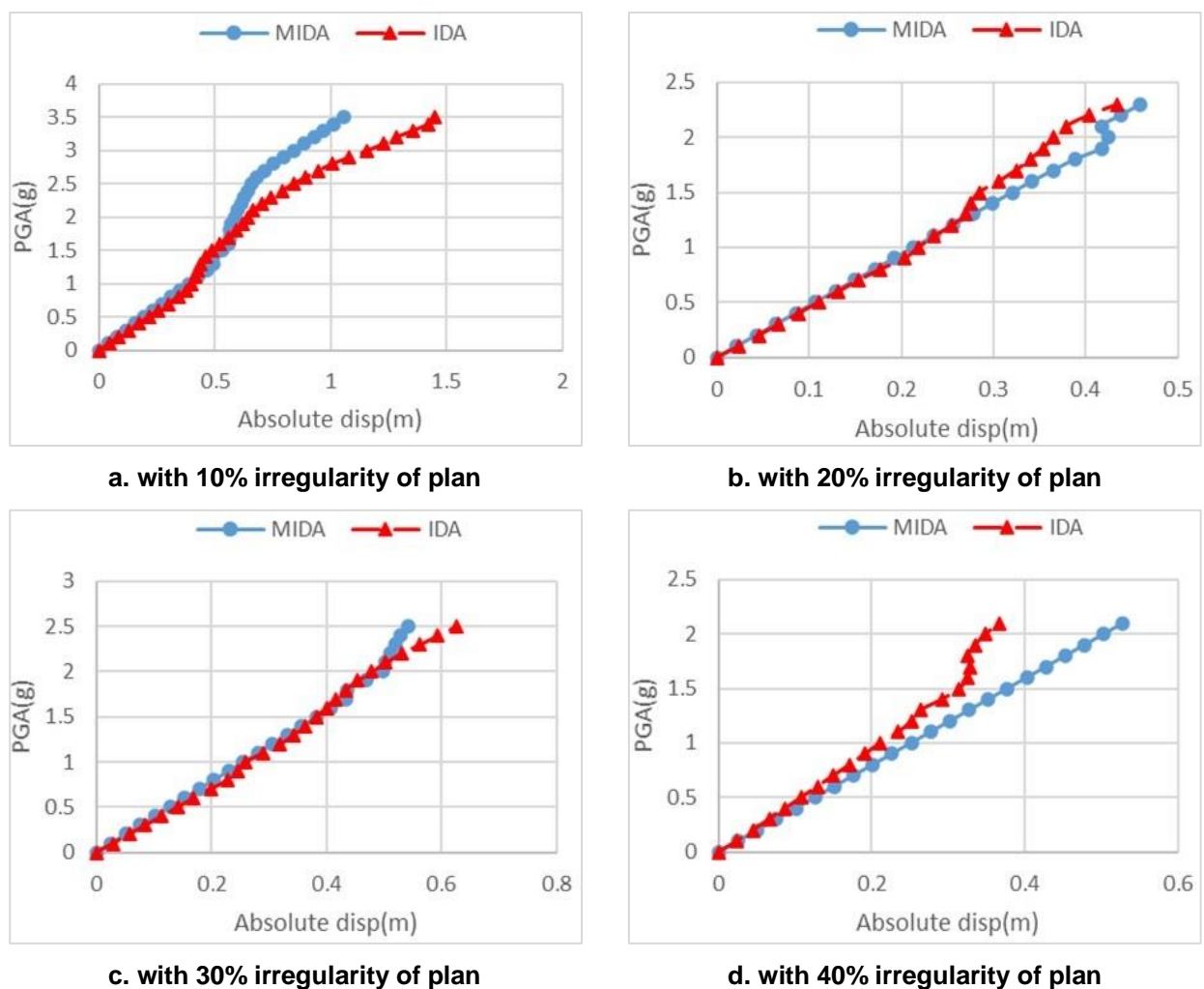


Figure 14. Comparison of roof displacement from IDA and MIDA methods in 18-storey structures under record No.3 in far field records Y-Direction.

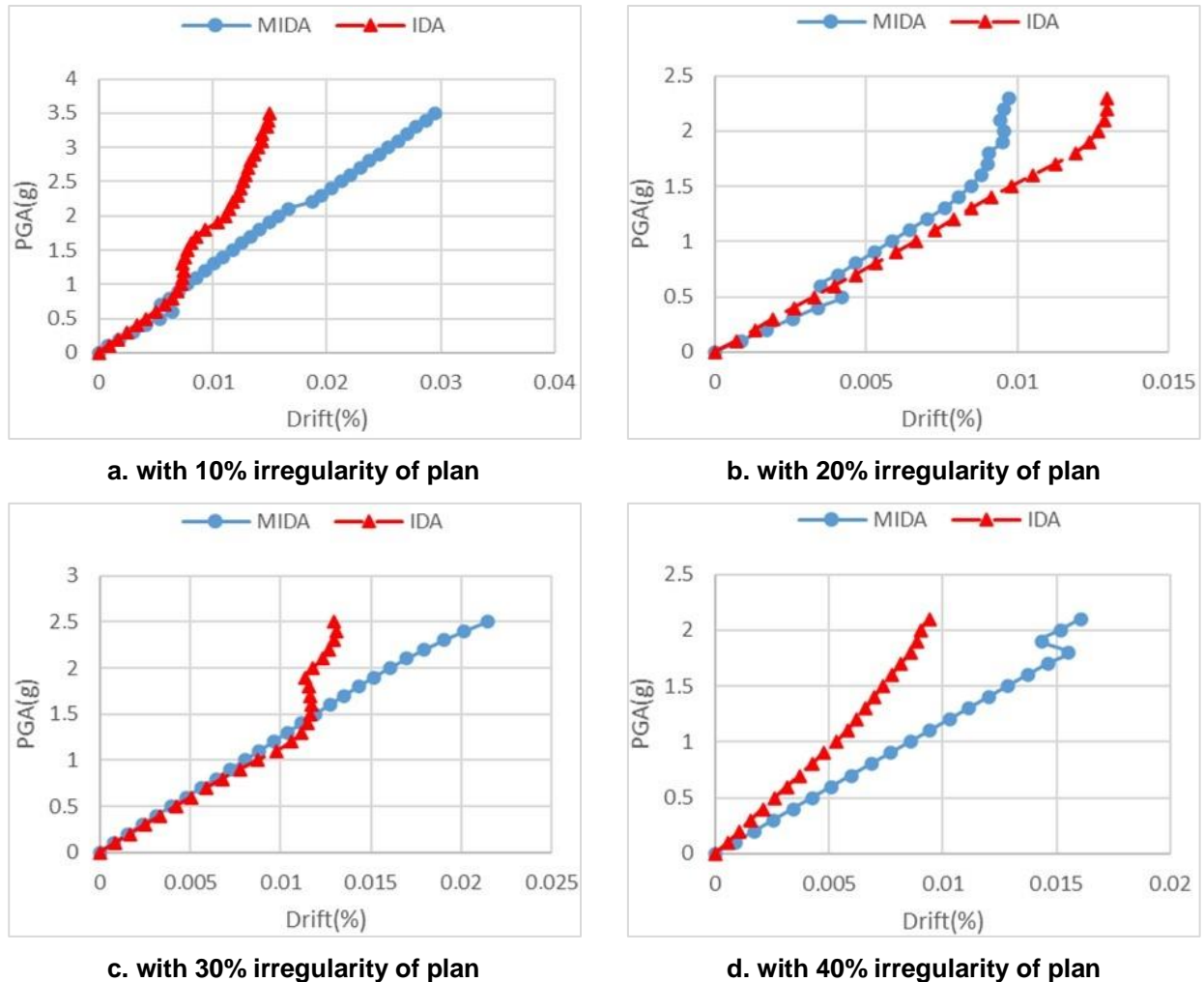


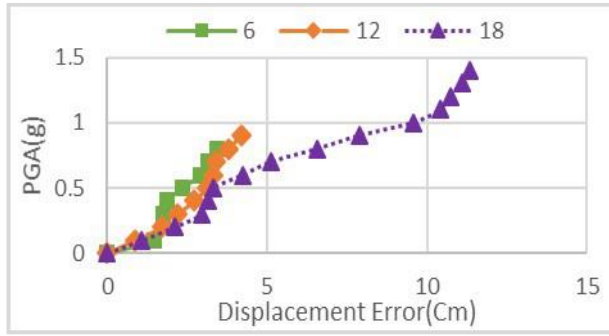
Figure 15. Comparison of roof drift from IDA and MIDA methods in 18-storey structures under record No.3 in far field records Y-Direction.

As Fig. 14 to Fig. 15 illustrate, MIDA method, in both maximum roof displacement and maximum roof drift, is capable of extracting the precise answer in linear region in far-field records. However, in nonlinear region, if the extent of intensity increases, errors of this method gradually increase in 18-storey structures. By passing the border of linear region in structural elements, they become plastic elements. Therefore, their stiffness changes; the periods of structures change accordingly. The validation of SRSS method is when modes do not have interference with each other. However, when structural elements become plastic and period changes, SRSS method is not valid anymore. Therefore, this is one of the factors creating some errors in this method in inelastic region. In addition, figures illustrate that if the extent of irregularity increases, errors of this method significantly increase because of the intense torsion of structure. Accumulation of plastic hinges in the reentrant corner of irregularity is the main reason of this effect. Therefore, applicability of this method narrows down.

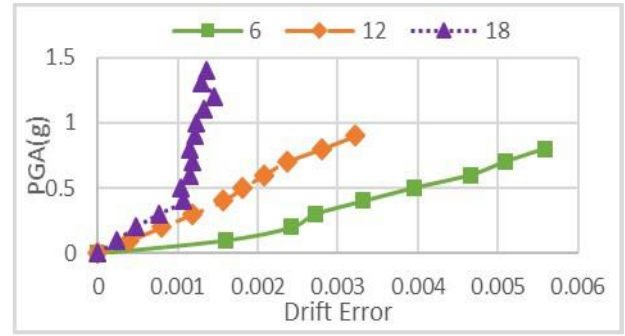
These errors are larger than those calculated in 6, 12-storey structures. Therefore, it can be deduced that when the height of structures increases, the considered modes should be increased by at least one more modes in order to decrease the errors in MIDA method.

3.1.3. Comparison of the effect of height and modes on maximum roof displacements' error as well as drifts' errors in fixed irregularities

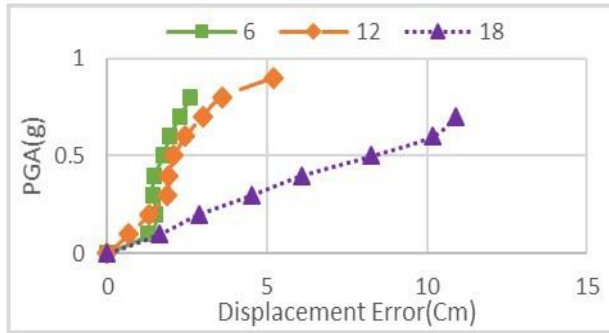
Comparison of the effect of height and modes on maximum roof displacements' error as well as drifts' error Versus PGA for average of structures' responses to 10 near-field records and 10 far-field records in fixed irregularities ranging from 10 % to 40 %.



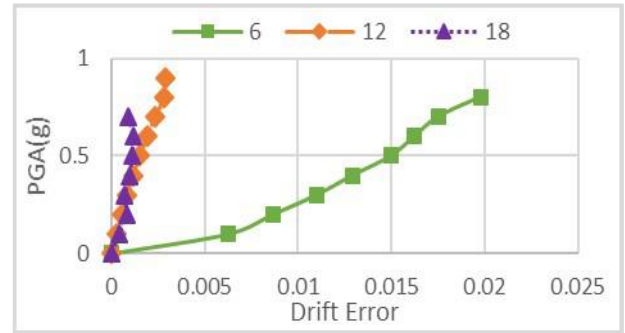
a. In structures with 10% irregularity on X-Direction



b. In structures with 10% irregularity on X-Direction

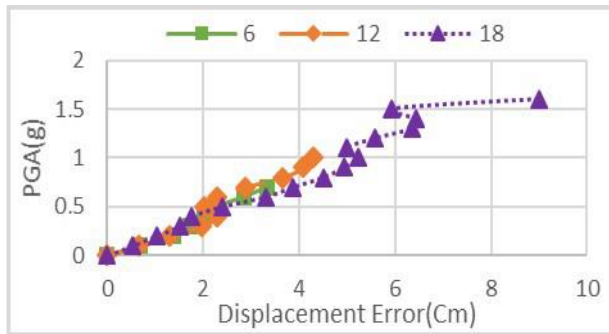


c. In structures with 20% irregularity on Y-Direction

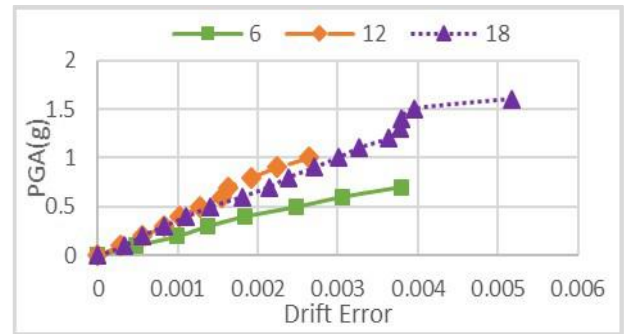


d. In structures with 20% irregularity on Y-Direction

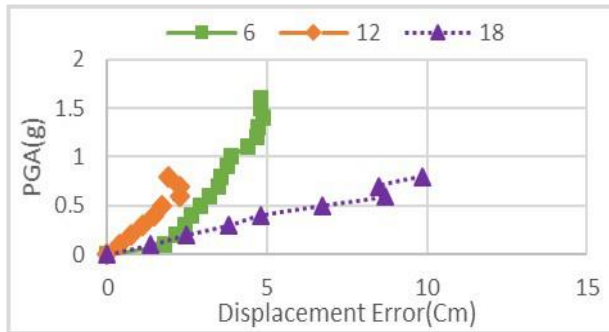
Figure 16. Comparison of the effect of height on roof displacement error and drift error between IDA and MIDA methods under average responses to far field records in structures with 10% and 20% irregularity.



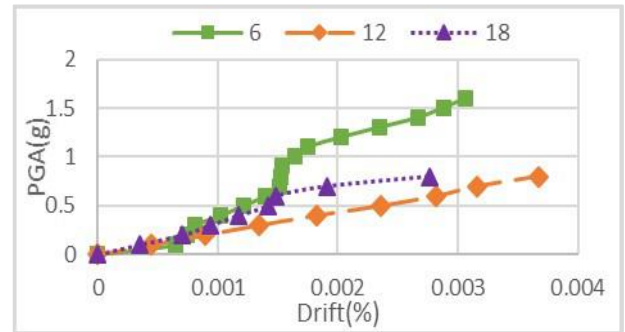
a. In structures with 30% irregularity which were recorded on X-Direction



b. In structures with 30% irregularity which were recorded on X-Direction



c. In structures with 40% irregularity which were recorded on Y- Direction



d. In structures with 40% irregularity which were recorded on Y- Direction

Figure 17. Comparison of the effect of height on roof displacement error and drift error between IDA and MIDA methods under average responses to far field records in structures with 30% and 40% irregularity.

Fig. 16(a) illustrates that 18-storey structures with irregularities of 10%, have the most errors in displacement despite considering one more mode in the 6 and 12-storey structures with irregularities of 10%. However, 6-storey structures with irregularities of 10% have the most errors in drift and 18-storey structures have the least errors, as shown in Fig. 16(b).

Fig. 16(c) illustrates that 18-storey structures with irregularities of 20%, have the most errors in displacement despite considering one more mode in the 6 and 12-storey structures with irregularities of 20%. Nevertheless, as depicted in Fig. 16(d), 6-storey structures with irregularities of 10% have the most errors in drift and 18-storey structures have the least.

3.2. Discussion

In this part, some discussions on results are explained in two main parts.

3.2.1. Discussion of near-field records

Special moment frames should satisfy allowable maximum drifts according to what exactly has been stated on the codes. In these frames, this criterion is dominant in designing structures and determining the dimensions of beams and columns. Therefore, this leads to an increase in beams and columns' cross-sections and consequently an increase in the stiffness of structures. In this type of frame, increasing the stiffness brings about a decrease in ductility; therefore, a decrease in the structures' periods. On the other hand, because these systems are used for their high ductility, they have higher period compared to the other lateral resisting systems. Krawinkler et al. (1999) [24] investigated the effect of specific pulses with the period of T_p on the responses of structures with a fundamental period of T at various performance levels. They found that SDOF spectra are adequate to represent multi-degree-of-freedom system ductility demands in stiff structures with $T/T_p < 1.0$, but are poor in representing the demands in flexible structures with $T/T_p > 1.0$ [24]. It was concluded that SDOF spectra alone are inadequate to represent seismic demands for near field earthquake ground motion [24]. As it is obvious, MIDA is a method based on the analysis of SDOF systems; hence MIDA method complies with what Krawinkler et al. stated in 1999 [24]. Hence, MIDA method is not valid in near-field earthquake records since this phenomenon is intensified in low-rise as well as medium rise structures. In addition, in near-field records movements, both PGA and PGV are very high. Their velocity somehow reaches about 100 cm/s to 200 cm/s . One of their characteristics is that they can dissipate huge quantities of energy in a very short period. Near-field records have a huge impact on low-rise structures. It can be inferred that MIDA method is not valid in the linear and nonlinear deformation as well as in low and mid-rise structures; but the results are much better in high-rise building because they get very little effect from near-field records compared to the others.

The pioneers of MIDA hypothesized modes operating separately from each other; but when structural elements pass the yielding point and become plastic, their stiffness decreases causing the interference of modes; therefore, SRSS method is not valid anymore. This is by far the most important factor that produces exceedingly large errors in nonlinear region.

As the extent of irregularity increases, errors of MIDA method dramatically increase owing to the intense torsion of structure. Accumulation of plastic hinges in the reentrant corner of irregularity is the main reason of this effect. Therefore, applicability of this method narrows down.

3.2.2. Discussion of far-field records

In these 12 structures, it is figuratively seen that the first mode has a dramatic direct effect on creation of the structures' displacement and the higher modes have a minor effect on creation of the structures' displacement. On the other hand, the higher modes have an immense direct effect on the creation of the drift and the first mode has a subtle effect on it. Therefore, the increase in considered modes in MIDA method, brings about a decrease in the errors of this method. Because 12-storey structures are higher than 6-storey structures, it is seen that the effect of higher modes on displacements and drifts of 2 stories below the roof are bigger than what is seen in 6-storey structures. Therefore, the errors in drift decrease. In 18-storey structures, by considering one more mode than 6 and 12-storey structures, the errors do not decrease to the expected level. Hence, for the 18-storey structures, it is perhaps better to consider at least two more modes.

3.2.3. Discussion on errors

1. Approximating the roof displacement versus base shear curve with bilinear curves brings about some errors in calculating drift and displacement.

2. The most important factor creating huge errors in nonlinear region is the modes interfering with each other. When structural elements pass the yielding point and become plastic, their stiffness decreases and this results in the interference of modes; therefore, SRSS method is not justifiable anymore. Therefore, the assumption of considering modes operating separately from each other is wrong.

3. Considering just the first two modes in each individual direction is one of the main causes of errors in 6 and 12-storey structures. A better alternative would be to consider more modes.
4. Regarding the errors of MIDA method, it is concluded in general:
 - Eigenvector (ϕ_{ji}) is not unique inherently. Therefore, $L_i = \sum m_j \phi_{ji}$ used in $(F_{yi})_{SDOF} = (F_{yi})_{MDOF} / (L/M)_i$ can cause this equation to have different answers and this would lead to wrong bilinear curve. Consequently, this can be the cause of errors in MIDA method.
 - As the extent of irregularity increases, displacement errors of this method significantly increase because of the intense torsion of structure. Accumulation of plastic hinges in the reentrant corner of irregularity is the main reason of this effect.
 - As the extent of irregularity increases, drifts' errors of this method significantly increase because of the intense torsion of structure. Therefore, in order to improve this method, there is a crucial need to introduce new damage index rather than drift in the procedure of MIDA.
 - There is no individual rule to figure out how many modes are enough and what optimum is to be considered in the procedure of MIDA.
 - In near-field records, low-rise structures are exposed to the effect of these earthquakes more than the others. SDOF spectra alone are inadequate to represent seismic demands for near field earthquake ground motion according to Krawinkler et al. (1999) [24]. It is evident that MIDA is a method based on the analysis of SDOF systems. Hence, MIDA method is not justifiable in near-field records as this phenomenon would cause too many errors in near-field records.

4. Conclusion

The obtained results of this research project are outlined below:

1. MIDA method is capable of calculating the damage indexes just as IDA method is.
2. As the extent of irregularity increases, applicability of this method narrows down.
3. In plan irregularity of structures, drift as damage index is not viable; therefore, there is a crucial need to improve this method through selecting new damage indexes.
4. Considering more modes for calculations in this method causes errors to decrease.
 - There is no individual rule to figure out how many modes are enough to be considered as optimum in the procedure of MIDA.
 - The speed of calculation in this method on 3D structures was amazing. There is a promising future ahead for future investigation of this method.
 - About the MIDA method, it can be said in general:
 - Transformation of 3D MDOF to an equivalent SDOF system reduces the time of calculation as well as CPU usage of computers.
 - Using the concept of pushover analysis in MIDA, all plastic hinges can be traced and the weak point of the structures can be detected in less time than IDA method.
 - Using the MIDA method in far-field records presents no difficulties. Therefore, it is highly recommended to employ this method.

Future researchers can carry out new surveys to consider other irregularities mentioned in ASCE7.

References

1. Bertero, V. Strength and deformation capacities of buildings under extreme environments. Structural Engineering and Structural Mechanics. 1977. 211–5.
2. Nassar, A., Krawinkler, H. Seismic demands for SDF and MDF systems. Report no. 95. p. 62–155: Stanford university: The John A. Blume Earthquake Engineering Center. 1991.
3. Bazzurro, P., Cornell, C. Seismic hazard analysis for non-linear structures. I: methodology. ASCE Journal of Structural Engineering. 1994. 120(11). 3320.
4. Mehanny, S., Deierlein, G. Modeling and assessment of seismic performance of composite frames with reinforced concrete columns and steel beams. Report no. 136: Stanford University: Blume Earthquake Engineering Center. 2000.
5. Gupta, B., Kunnath, S. Adaptive spectra-based pushover procedure for seismic evaluation of structures. Earthquake spectra. 2000. 16(2). Pp. 367–392.
6. Vamvatsikos, D., Cornell, C.A. Direct estimation of seismic demand and capacity of multidegree-of-freedom systems through incremental dynamic analysis of single degree of freedom approximation. Journal of Structural Engineering. 2005. 131(4). Pp. 589–599.

7. Khorami, M., Alvansazyazdi, M., Shariati, M., Zandi, Y., Jalali, A., Tahir, M. Seismic performance evaluation of buckling restrained braced frames (BRBF) using incremental nonlinear dynamic analysis method (IDA). *Earthquake and Structures*. 2017. 13. Pp. 531–538. DOI: 10.12989/eas.2017.13.6.531
8. Davani, M.R., Hatami, S., Zare, A. Performance-based evaluation of strap-braced cold-formed steel frames using incremental dynamic analysis. *Steel and Composite Structures*. 2016. Vol. 21. No. 6. Pp. 1369–1388. DOI: 10.12989/scs.2016.21.6.1369
9. Bayat, M., Daneshjoo, F., & Nistico, N. A novel proficient and sufficient intensity measure for probabilistic analysis of skewed highway bridges. *Structural Engineering and Mechanics*. 2015. 55(6). Pp. 1177–1202. DOI: 10.12989/SEM.2015.55.6.1177
10. Mofid, M., Zarfam, P., Fard, B. On the modal incremental dynamic analysis. *The Structural Design of Tall and Special Buildings*. 2005. 14. Pp. 315–329.
11. Han, S., Chopra, A. Approximate incremental dynamic analysis using the modal pushover analysis procedure. *Engineering Structural Dynamics*. 2006. 35(15). Pp. 1853–1873.
12. Zarfam, P., Mofid, M. Evaluation of modal incremental dynamic analysis, using input energy intensity and modified bilinear curve. *The Structural Design of Tall and Special Buildings*. 2008. 18. Pp. 573–586.
13. Zarfam, P., Mofid, M. On the modal incremental dynamic analysis of reinforced concrete structures, using a trilinear idealization model. *Journal of Engineering Structures*. 2011. 33. Pp. 1117–1122.
14. Shafei, B., Zareian, F., Lingos, D.G. A simplified method for collapse capacity assessment of moment-resisting frame and shear wall structural systems. *Engineering Structures*. 2011. 33(4). Pp. 1107–1116. DOI: 10.1016/j.engstruct.2010.12.028
15. Jalilkhani, M., Manafpour, A.R. Evaluation of seismic collapse capacity of regular RC frames using nonlinear static procedure. *Structural Engineering and Mechanics*. 2018. 68(6). Pp. 647–660. DOI: 10.12989/SEM.2018.68.6.647
16. Zafarkhah, E., Keipour, N., Mofid, M. Exerting Modal Incremental Dynamic Analysis (MIDA) in surveying seismic Behavior of structures Equipped by Self-Centering viscoelastic Damper. *Journal of Vibroengineering*. 2017. 19(2). Pp. 783–800.
17. Bergami, A.V., Forte, A., Lavorato, D. Proposal of a Incremental Modal Pushover Analysis (IMPA). *Earthquakes and Structures*. 2017. Vol. 13. No. 6. Pp. 539–549.
18. ASCE07. Minimum design loads for building and other structures. American Society of Civil Engineers: Washington DC, USA. 2010.
19. AISC360. Specification for structural steel buildings, AISC 360. An American National Standard Institute: Washington DC, USA. 2010.
20. FEMAP695. Quantification of Building Seismic Performance Factors. the Applied Technology Council for the Federal Emergency Management Agency: Washington DC, USA. 2009.
21. Dimakopoulou, V., Fragiadakis, M., Spyrakos, C. Influence of modeling parameters on the response of degrading systems to near-field ground motions. *Journal of Engineering Structures*. 2013. 53. Pp. 10–24.
22. Davoodi, M., Jafari, M., Hadiani, N. Seismic response of embankment dams under near-fault and far-fault ground motion excitation. *Journal of Engineering Geology*. 2013. 158. Pp. 66–76.
23. FEMA356. Prestandard and Commentary for the Seismic Rehabilitation of Buildings, FEMA 356. Federal Emergency Management Agency: Washington DC, USA. 2000.
24. Gala, K., Ghobarah, A. Effect of near-fault earthquakes on North American nuclear design spectra. *Nuclear Engineering and Design*, Elsevier. 2006. 236(18). Pp. 1928–1936.

Contacts:

Hamidreza Mehdipanah, hmehdipanah@mail.kntu.ac.ir.

Nader Fanaie, fanaie@kntu.ac.ir

© Mehdipanah, H.R., Fanaie, N., 2021